ORIGINAL ARTICLE

Redox conditions and pH control trace element concentrations in a meandering stream and shallow groundwater of a semiarid mountain watershed, Red Canyon, Wyoming, USA

Gregory T. Carling[1] · Edwin A. Romanowicz[2] · Li Jin[3] · Diego P. Fernandez[4] · David G. Tingey[1] · Timothy H. Goodsell[1]

Abstract

The interface between oxic surface water and anoxic groundwater plays an important role in trace element cycling in mountains streams. In this investigation, stream water and shallow groundwater were sampled in a semiarid mountain catchment at Red Canyon, Wyoming, USA to evaluate variability in redox conditions and trace element concentrations. Samples were collected in July 2013 during summer baseflow conditions and in May 2014 during snowmelt runoff. Field measurements showed dissolved oxygen-saturated stream water and anoxic groundwater, with relatively higher pH in surface water. Groundwater and surface water chemistry were remarkably similar during both the summer and spring sampling events, indicating overall stability of the oxic/anoxic transition and trace element concentrations. Similar stable water isotope values indicate a close connection between the surface water and groundwater (δ^{18}O and δD ranged from -18.1 to $-18.9‰$ and from -140 to $-147‰$, respectively). Concentrations of most trace and major elements were a factor of two higher in groundwater relative to surface water. Notably, Mn, Fe, and Ce concentrations were 7–90-fold higher in groundwater relative to surface water. In contrast, As, Se, and V concentrations were 3–30-fold lower in groundwater relative to surface water, likely due to pH- and redox-driven changes in speciation and sorption. This study is important for characterizing trace element cycling in mountainous areas, where measurements are rare, and has implications for furthering understanding of the key biogeochemical processes that occur during groundwater–surface water interactions.

Keywords Groundwater–surface water interactions · Mountain hydrology · Redox · Trace elements · Red Canyon · Wyoming

✉ Gregory T. Carling
  greg.carling@byu.edu

1   Department of Geological Sciences, Brigham Young University, Provo, UT, USA

2   Center for Earth and Environmental Sciences, State University of New York at Plattsburgh, Plattsburgh, NY, USA

3   Department of Geology, State University of New York College at Cortland, Cortland, NY, USA

4   Department of Geology and Geophysics, University of Utah, Salt Lake City, UT, USA

Introduction

The reduction/oxidation (redox) boundary between groundwater and surface water in stream systems is a hotspot of biogeochemical cycling. Chemical oxidation/reduction and solution pH both control groundwater composition beyond dilution and mixing (Siegel 2008). Abrupt transitions between oxidizing surface water and reducing groundwater combined with changes in pH can alternately mobilize or immobilize trace elements during hyporheic exchange (Nagorski and Moore 1999). Redox conditions are often linked to the occurrence of contaminants such as As in groundwater (McMahon and Chapelle 2008; Smedley and Kinniburgh 2002). Significant questions still remain about how redox conditions affect trace element cycling and the potential impacts on water quality. Mountain watersheds are particularly important for study due to climate-driven decreases in snowpack, which may lead to a decline in

groundwater recharge and stream discharge (Meixner et al. 2016).

The purpose of this study is to investigate trace element behavior in a meandering stream and adjacent groundwater in a semiarid mountain stream in a seasonally snow-covered watershed at Red Canyon, Wyoming. Red Canyon Creek watershed has been well studied over the past decade for hydrology and water chemistry (Bauer et al. 2009; Fanelli and Lautz 2008; Jin et al. 2009, 2010, 2012; Lautz and Fanelli 2008; Lautz and Siegel 2006, 2007; Lautz et al. 2006). This study builds upon the previous work by including measurements of trace element and redox chemistry in groundwater and surface water. Specific objectives are to (1) compare trace element concentrations in surface water and groundwater, (2) evaluate spatial variability in groundwater chemistry, and (3) evaluate seasonal variability from summer baseflow to spring runoff.

Materials and methods

Field area

Red Canyon Creek watershed is located on the southeastern flank of the Wind River Range in Wyoming, USA (Fig. 1). The watershed has an area of ~ 80 km^2 and ranges in elevation from ~ 1700 to ~ 2700 m above sea level. The normal annual precipitation is 40 cm, of which 60% falls during the months of October through April, primarily in the form of snow (NOAA 2016). The mean annual air temperature is 7.3 °C, with a long-term mean annual daily minimum of 0.5 °C and maximum of 14.1 °C (NOAA 2016). The watershed contains several ephemeral streams and the perennial

Cherry Creek and Red Canyon Creek, which join near the confluence with the Little Popo Agie River at the base of the watershed. Red Canyon is underlain by eastward dipping sedimentary beds of the Paleozoic-age Madison Limestone, Tensleep Sandstone, Amsden Formation, and Phosphoria Formation and the Mesozoic-age Chugwater and Dinwoody Formations and Nugget Sandstone.

The study area is located at the base of the watershed with samples collected in meandering sections at a moderate-relief meadow in Cherry Creek and a low-relief meadow on Red Canyon Creek (Fig. 1). The meadow at Red Canyon Creek is underlain by 6–7 m of unconsolidated alluvium. Silty sands extend from the ground surface to a depth of about 2 m, where there is a discrete layer of highly permeable sand and gravel (hydraulic conductivity ranging from 3×10^{-4} to 10^{-3} cm/s) that extends to the relatively impermeable bedrock of the Chugwater Formation (Lautz and Siegel 2006). The site is instrumented with over 30 shallow wells and piezometers as a part of hydrogeologic investigations of the University of Missouri–Columbia's Branson Geology field camp (Bauer et al. 2009; Lautz et al. 2006). Wells and piezometers range in depth from 2 to 3 m below ground surface. At the Red Canyon meadow, groundwater is recharged by a losing section of the stream at the top of the meander and returns to the stream at a gaining section at the bottom of the meander (Lautz and Siegel 2006). Groundwater travel times are estimated at several years across the meadow (Lautz and Siegel 2006).

Six representative wells in the Red Canyon Creek meadow and one well in the Cherry Creek meadow were selected for sampling, along with surface water samples at two sites on Red Canyon Creek and one site on Cherry Creek (Fig. 1). Field sampling was conducted on 14–15

Fig. 1 Study area in Red Canyon, Wyoming, USA, showing Cherry Creek and Red Canyon Creek on the southeastern end of the Wind River Range (WRR). Groundwater and surface water sample locations are shown as blue circles and red squares, respectively. Particle pathlines are modified after Lautz and Siegel (2006), who developed a MODFLOW and MT3D model for the experimental reach on Red Canyon Creek. Base images from ESRI
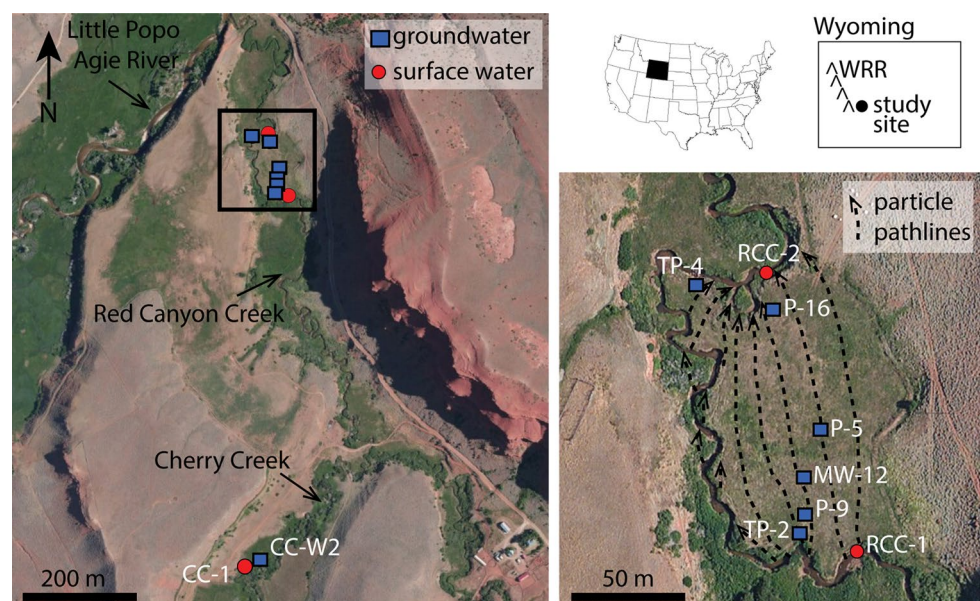
July 2013 during summer baseflow conditions and 2 May 2014 during spring snowmelt runoff. A total of three surface water and seven groundwater samples were collected during each season. Snow telemetry (SNOTEL) data from nearby Townsend Creek station indicate that the May sampling period occurred during the primary snowmelt season in the headwaters of Red Canyon Creek (Fig. 2). Red Canyon wells were selected along the hydraulic gradient as illustrated by MT3D-generated particle pathlines for groundwater beneath the meadow (Lautz and Siegel 2006) (Fig. 1). The groundwater flow direction beneath the Cherry Creek meadow is unclear, but there is likely flow between the meanders with additional flow upgradient from the east.

Sample collection

Samples were collected from shallow groundwater and surface water using standard methods (USEPA 1996). Water was pumped through Teflon tubing using a Geopump peristaltic pump with a short section of MasterFlex tubing at the pump head. The tubing was cleaned prior to collecting each sample by pumping 10% v/v HCl through the tubing for several minutes followed by rinsing with excessive amounts of Milli-Q water. Field parameters, including dissolved oxygen, oxidation–reduction potential (ORP), water temperature, pH, and conductivity, were measured using a YSI Quatro multiparameter probe that was calibrated at the beginning of each sampling day. For surface water samples, field parameters were measured by placing the probe directly in the stream below the sample collection point. For groundwater samples, and field parameters were measured using a flow-through cell and purging the wells until field parameters stabilized.

Filtered water samples were collected by passing water through an inline 0.45 μm PES cartridge filter to a prerinsed
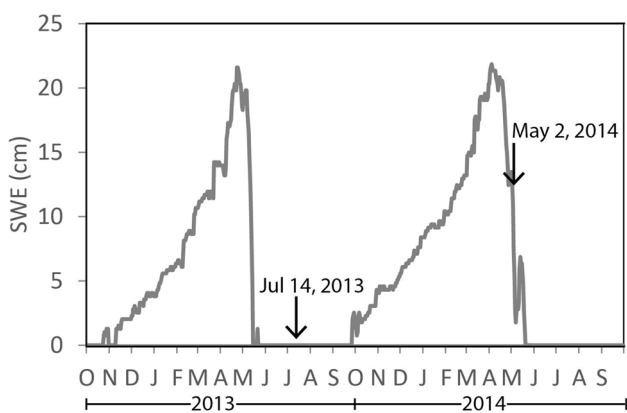

Fig. 2 Snow water equivalent (SWE) data from Townsend Creek snow telemetry (SNOTEL) station for the 2013 and 2014 water years. Arrows indicate sample dates at Red Canyon watershed

30 mL LDPE bottle for major anion measurements and an acid-washed and preacidified (2.4% v/v HNO_3) 60 mL LDPE bottle for trace element and major cation measurements. After collecting the filtered samples, the cartridge filter was removed and an unfiltered sample was collected in a 1 L LDPE bottle for measurements of bicarbonate and stable isotopes in water (δD and $\delta^{18}O$). To test for possible contamination during sample collection, transport, and storage, one field blank was collected during each sampling day (total of three field blanks). The field blank samples were collected using clean tubing to pump Milli-Q water from a 1 L LDPE bottle to 30 mL and 60 mL bottles for anion and trace element/cation measurements, respectively.

Laboratory analysis

Trace element and major cation concentrations were measured with a quadrupole inductively coupled plasma mass spectrometer (ICP-MS) (USEPA 1994). We used an Agilent 7500ce ICP-MS with a collision cell, a double-pass spray chamber with perfluoroalkoxy (PFA) nebulizer (0.1 mL/min), a quartz torch, and platinum cones. Concentrations were measured for the following 40 elements: Ag, Al, As, B, Ba, Be, Ca, Cd, Ce, Co, Cr, Cs, Cu, Dy, Fe, Gd, Ho, K, La, Li, Lu, Mg, Mn, Mo, Na, Nd, Ni, Pb, Rb, Sb, Se, Sm, Sr, Tb, Ti, Tl, U, V, Y, and Zn. A calibration solution containing all the elements reported was prepared gravimetrically using 1000 mg/L single-element standards (Inorganic Ventures, Inc.). This solution was used to prepare a calibration curve with six points plus a blank for each sample run. Al, Ca, Cr, Fe, K, Mn, Na, and V were determined using 4 mL He/min in the collision cell, As and Se were determined using 4 mL He/min plus 2.5 mL H_2/min, and the other 30 elements were determined using Ar as the carrier gas. Detection limit (DL) was determined as three times the standard deviation of all blanks analyzed throughout each run. A USGS standard reference sample (T-205) and NIST standard reference material (SRM 1643e) were analyzed multiple times in each run together with the samples as a continuing calibration verification. The long-term reproducibility for T-205 and SRM 1643e shows that our results are consistently accurate within 10% for most elements.

Major anions (Cl^-, NO_3^-, and SO_4^{2-}) were analyzed on filtered aliquots using a Dionex ICS-90 ion chromatograph (USEPA 1997), and alkalinity (assumed to be HCO_3^-) was measured using a Mettler Toledo DL50 titrator with dilute HCl (USEPA 1978). Stable isotopes in water (δD and $\delta^{18}O$) were measured on unfiltered aliquots using a Los Gatos Research Liquid Water Isotope Analyzer (LWIA-24d) (Newman et al. 2009). All measurements were made relative to Vienna Standard Mean Ocean Water (VSMOW), with a precision of 1.0‰ and 0.4‰ for δD and $\delta^{18}O$, respectively.

Data quality control

Field blanks showed low background concentrations for all measured elements, with concentrations < DL in nearly all cases. Ca, K, and Li had measureable values in at least one of the three field blanks, but the concentrations were negligible relative to concentrations measured in actual samples. Concentrations of all other elements were < DL in the field blanks. Another set of 18 elements had concentrations < DL in the field blanks and in most samples, including Ag, Al, Be, Cd, Cr, Cs, Cu, Dy, Gd, Ho, La, Lu, Nd, Pb, Sb, Sm, Tb, and Tl, and thus were removed from the dataset for all further analyses. For other elements, any values < DL were set as 1/2 DL.

Charge balances, calculated using cation (K^+, Na^+, Ca^{2+}, Mg^{2+}) concentrations from the ICP-MS, anion (Cl^-, NO_3^-, SO_4^{2-}) concentrations from the IC, and HCO_3^- concentrations from titration, were within ± 5% for 18 out of 20 samples and − 5.3% and − 6.3% for the other two samples (Supplementary material, Table S1).

Geochemical modeling

Saturation indices (SI) and aqueous speciation were calculated with PHREEQC using the Minteq.v4 thermodynamic database (Parkhurst and Appelo 1999). Positive SI values indicate oversaturation and potential for mineral precipitation. The distribution of elements among their valence states was calculated using field-measured pH and calculated pe values, which were estimated using dissolved oxygen concentrations for surface water and the Fe(II)/Fe(III) redox couple for groundwater. We assumed that Fe measured on filtered samples was Fe(II) and used a nominal value of 1 μg/L for Fe(III) concentrations. These input values resulted in pe values > 12 for surface water and pe values ranging from 0.5 to 3.3 for groundwater.

Results

Groundwater and surface water stable isotope composition

Stable isotopes in water (δD and $δ^{18}O$) showed minimal seasonal variability in both groundwater and surface water (Fig. 3). Surface water samples had nearly identical isotopic composition in samples collected 14–15 July 2013 and 2 May 2014. Groundwater samples showed greater variability between sampling periods relative to surface water, with δD values slightly more depleted in samples collected in May relative to samples collected in July. However, the variability in δD was small (~ 3‰) and some of the May samples overlap in isotopic space with the July samples.
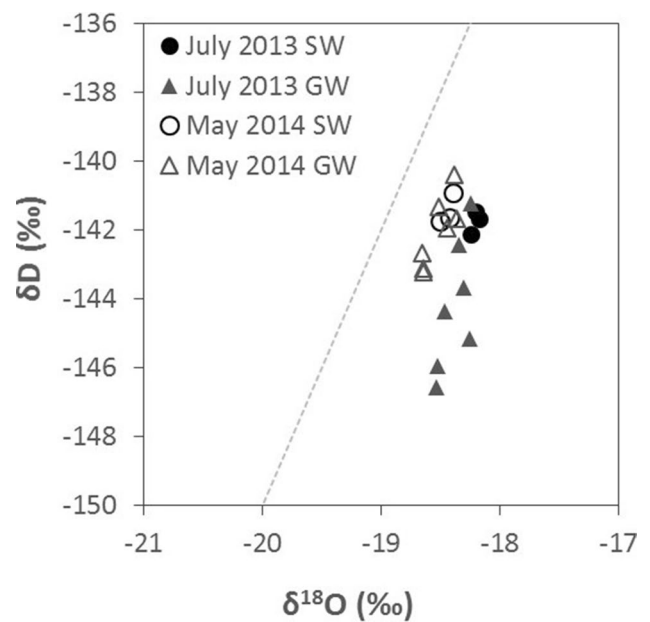

Fig. 3 Stable isotope composition of surface water (SW) and groundwater (GW) for samples collected 14–15 July 2013 and 2 May 2014. The dashed line is the global meteoric water line

Groundwater and surface water chemistry

Field parameters indicated dramatically different water chemistry between surface water and groundwater (Fig. 4). Specifically, dissolved oxygen, ORP, water temperature, and pH were higher in surface water relative to groundwater. Dissolved oxygen was > 80% of saturation in surface water and were negligible in groundwater. Likewise, ORP values were mostly positive in surface water and negative in groundwater samples. The exceptions were wells MW-12 and CC-W2, which had slightly positive ORP values in July and May samples, respectively. Temperature was higher overall in surface water relative to groundwater, with warmer temperatures in July 2013 relative to May 2014 for both groundwater and surface water. The pH was > 8 in surface water and circumneutral (~ 7) in groundwater.

Major solute concentrations and conductivity were on average ~ 50% higher in groundwater relative to surface water (Fig. 4). Well CC-W2 had the highest conductivity (with values over 1500 μS/cm), which was nearly three times higher than the conductivity of surface water. Ca, SO_4, and Sr behaved similarly as conductivity, with slightly higher concentrations in groundwater relative to surface water, and with the highest concentrations in well CC-W2 (Fig. 4). Other major solutes and conservative trace elements showed similar trends as conductivity (Supplementary material, Table S1).

Specific redox-sensitive trace elements had very different concentrations between surface water and groundwater
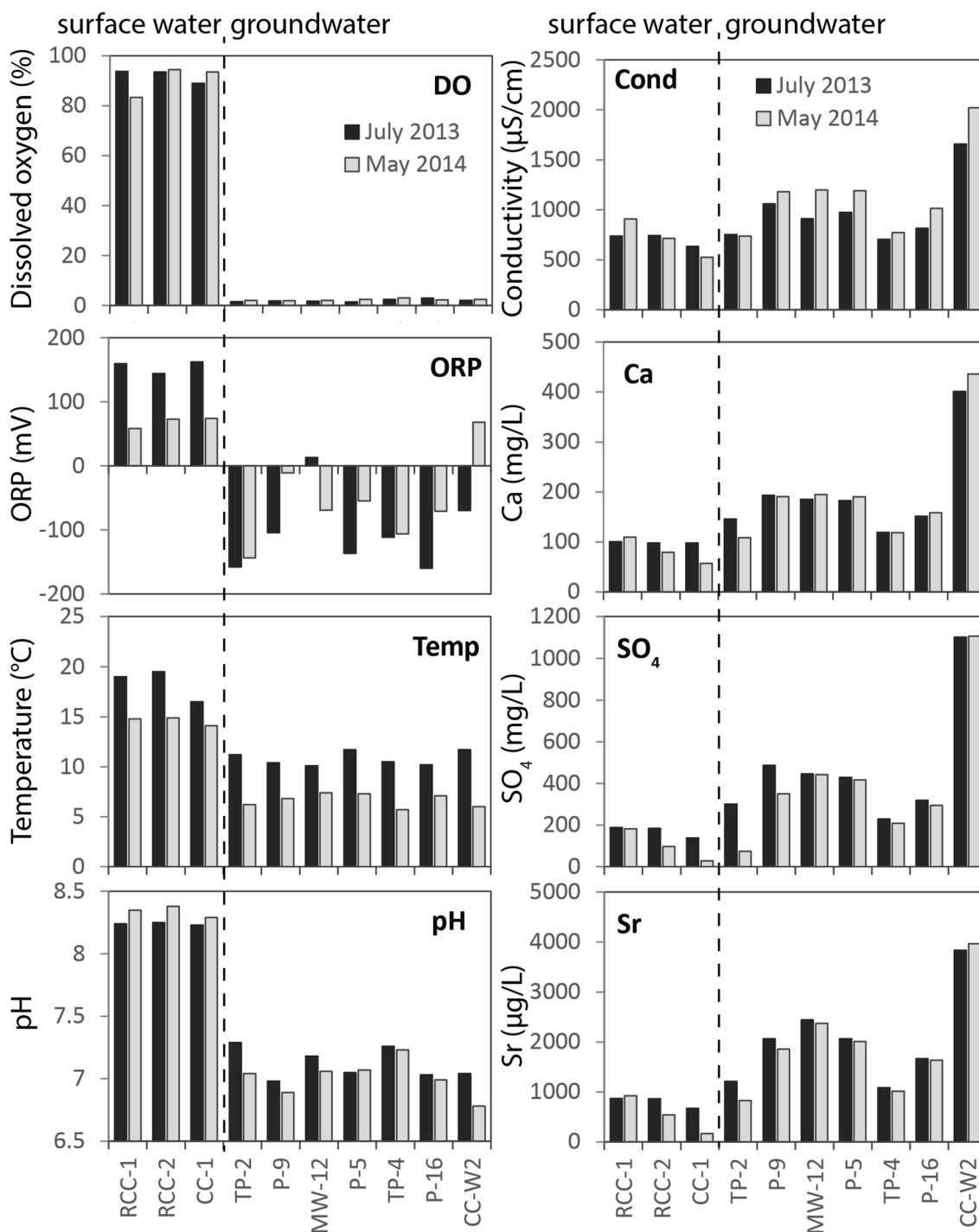
Fig. 4 Field parameters dissolved oxygen (%), oxidation–reduction potential (ORP, mV), temperature (°C), pH, conductivity (µS/cm), and concentrations of Ca (mg/L), SO_4 (mg/L), and Sr (µg/L) in surface water and groundwater samples collected 14–15 July 2013 and 2

May 2014. Dissolved oxygen, ORP, pH, and temperature values were typically higher in surface water, whereas conductivity, Ca, SO_4, and Sr concentrations were typically higher in groundwater

(Fig. 5). On average, Fe concentrations were ~ 90 times higher in groundwater relative to surface water, Mn concentrations were ~ 20 times higher, and Ce concentrations were ~ 7 times higher. However, concentrations were spatially variable, especially considering well MW-12, which had low concentrations of Fe, Mn, and Ce. Well CC-W2 had relatively low Fe concentrations with high Mn
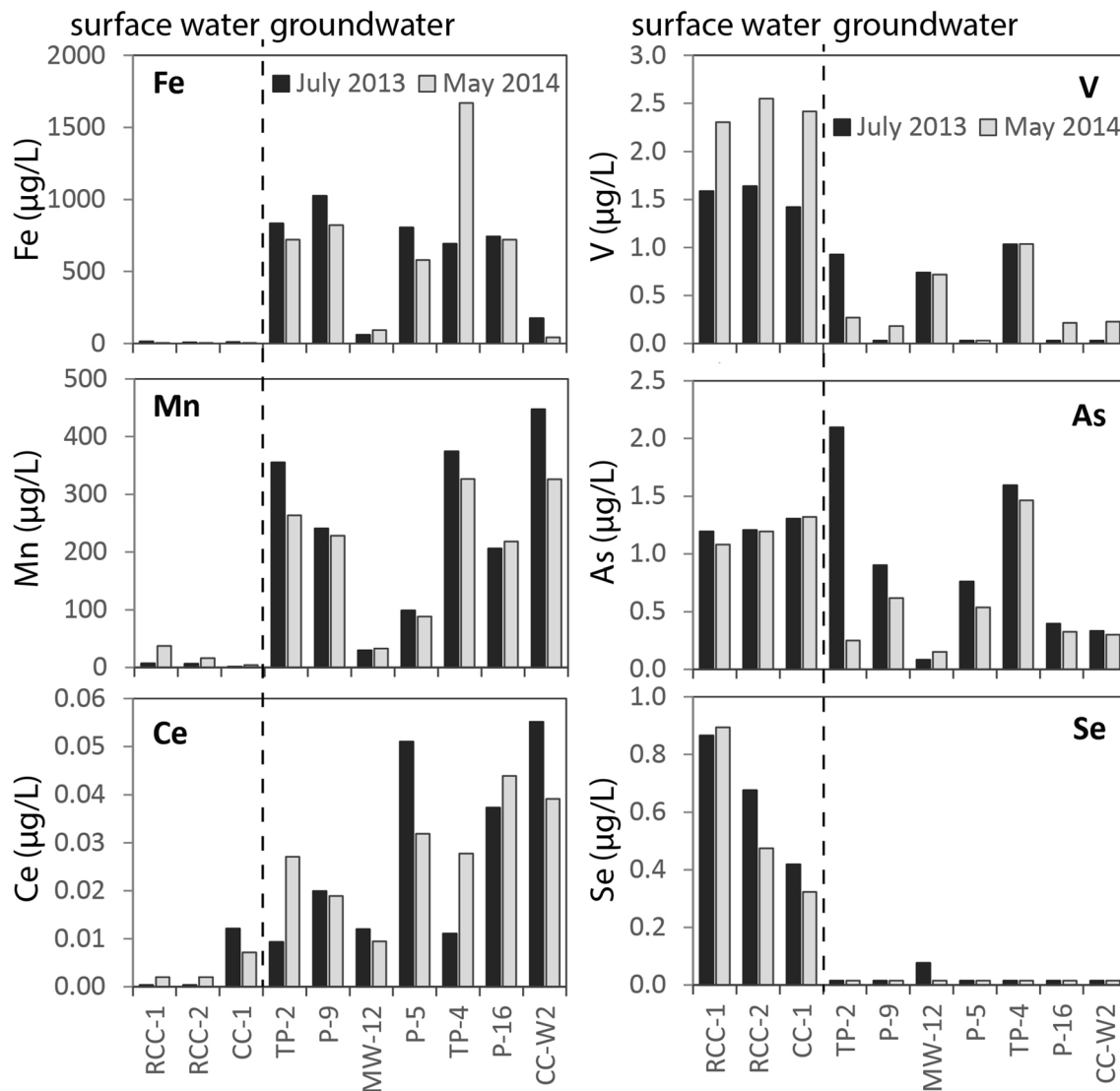
Fig. 5 Trace element (Mn, Fe, Ce, As, V, and Se) concentrations (µg/L) in surface water and groundwater samples collected 14–15 July 2013 and 2 May 2014. Fe, Mn, and Ce concentrations were typi-cally higher in groundwater, whereas V, As, and Se concentrations were typically higher in surface water

and Ce concentrations, whereas well P-5 had moderate Mn concentrations with high Fe and Ce concentrations.

In contrast to Mn, Fe, and Ce, concentrations of specific oxyanion-forming elements, including Se, V, and As, were higher in surface water relative to groundwater (Fig. 5). On average, Se concentrations were ~30 times higher in surface water relative to groundwater and V concentrations were 5 times higher. Se concentrations were low in all groundwater samples, whereas V concentrations were more variable with moderate concentrations in wells MW-12 and TP-4. Vana-dium also showed seasonal variability in surface water, with higher concentrations in May 2014 relative to July 2013. Arsenic concentrations were also relatively higher in surface water samples relative to groundwater with the exception of

well TP-2 during July 2013 and well TP-4 during both July 2013 and May 2014. Wells P-5 and P-9 had moderate As concentrations, whereas wells MW-12, P-16, and CC-W2 had low As concentrations.

Geochemical modeling

PHREEQC-calculated speciation and saturation indices showed different conditions between surface water and groundwater for specific redox-sensitive elements and min-eral phases (Table 1). Selenium and V were predicted as SeO_4^{2-} (+VI oxidation state) and $H_2VO_4^-$ or HVO_4^{2-} (+V oxidation state) in surface water and as $HSeO_3^-$ (+IV oxida-tion state) and $V(OH)_3$ (+III oxidation state) in groundwater,

Table 1 Geochemical modeling inputs and results

	Groundwater	Surface water
pH	6.78–7.29	8.23–8.38
calculated pe	0.5–3.3	12.2–12.4
V speciation	$V(OH)_3$ (+III oxidation state)	$H_2VO_4^-$ or HVO_4^{2-} (+V oxidation state)
As speciation	$HAsO_4^{2-}$ (+V oxidation state)	$HAsO_4^{2-}$ (+V oxidation state)
Se speciation	$HSeO_3^-$ (+IV oxidation state)	SeO_4^{2-} (+VI oxidation state)
Minerals with positive saturation index (SI > 0)	Aragonite, calcite, dolomite, birnessite, bixbyite, ferrihydrite, goethite, hematite	FeSe, $FeSe_2$, elemental Se

respectively. Arsenic was predicted as $HAsO_4^{2-}$ (+V oxidation state) in both surface water and groundwater. Surface water was oversaturated with respect to carbonate minerals (aragonite, calcite, and dolomite) and Fe- and Mn oxides (including birnessite, bixbyite, ferrihydrite, goethite, and hematite). In contrast, groundwater was undersaturated or at equilibrium with respect to many carbonate minerals and Fe- and Mn oxides. Notably, groundwater was oversaturated with respect to Se-bearing mineral phases including FeSe, $FeSe_2$, and elemental Se.

Discussion

Redox conditions and pH control groundwater and surface water chemistry

Redox conditions and pH are important controls on groundwater and surface water chemistry in Red Canyon Creek watershed. Elevated Mn and Fe concentrations in groundwater (Fig. 5) are likely the result of reductive dissolution of Mn- and Fe oxides and oxyhydroxides from the aquifer material (Chapelle and Lovley 1992). Mn- and Fe-bearing minerals were oversaturated in surface water, suggesting that these minerals precipitate out of solution when groundwater is oxidized during groundwater–surface water exchange. Elevated Ce concentrations in groundwater are also likely related to redox conditions, since reduced forms of Ce are more soluble (Vázquez-Ortega et al. 2015). Although Ce thermodynamic data were not available for geochemical modeling in PHREEQC, groundwater likely contains more soluble Ce(III) species, whereas surface water likely contains less soluble Ce(IV) species.

In contrast to cation-forming elements, concentrations of the oxyanion-forming elements Se, V, and As were higher in surface water relative to groundwater (Fig. 5). Vanadium and Se concentrations in our samples were positively correlated with pH ($R^2 > 0.80$), with the lower pH of groundwater likely promoting sorption of oxyanion species (Carling et al. 2011; Dzombak and Morel 1990). Lower pH in groundwater may also contribute to the lower As concentrations observed

in most samples by promoting sorption (Dicataldo et al. 2011). Notably, the decrease in pH between surface water and groundwater is likely driven by calcite precipitation in response to gypsum dissolution due to the common ion effect, as reported from the previous work in the watershed (Jin et al. 2010). Elevated As concentrations in well TP-4, which also had relatively high Fe and Mn concentrations, may be the result of co-dissolution of As during reductive dissolution of Mn- and Fe oxides and oxyhydroxides (Haque et al. 2008).

Selenium concentrations in groundwater may also be associated with redox conditions or mineral precipitation. The geochemical modeling results predicted different redox states for these elements in surface water and groundwater (Table 1). For example, the reduced selenite species of Se predicted by PHREEQC in groundwater have a higher tendency for sorption in groundwater relative to the oxidized selenate species in surface water (Dzombak and Morel 1990). Low Se concentrations in groundwater may be further explained by precipitation of Se-bearing minerals such as FeSe and $FeSe_2$, which were predicted to be oversaturated in groundwater samples (Table 1).

Spatial variability in groundwater redox chemistry

Variability in groundwater redox chemistry affects the trace element chemistry in the wells. For example, Fe and Mn concentrations and ORP across the wells (Figs. 4, 5). This suggests that redox conditions are spatially variable in groundwater with zones of dominant Mn- or Fe reduction driven by variability in physical properties and geochemical composition of the aquifer material. Anoxic conditions are present in groundwater in close proximity to the stream, as indicated by well TP-2, which had low dissolved oxygen and high Fe and Mn concentrations. Well CC-W2 had high Mn concentrations but low Fe concentrations, with ORP values near zero, suggesting variability in Mn and Fe reduction processes in the groundwater system. Well MW-12 was the least reducing of all groundwater samples with relatively low Mn and Fe concentrations and ORP values near zero. Notably, well MW-12 also had relatively high V concentrations, illustrating

the importance of redox state for controlling the chemistry of specific trace elements, as they may be less likely to adsorb to aquifer sediments under oxidizing conditions. Based on our measurements, dissolved oxygen concentrations are useful for determining oxic versus anoxic conditions, but are not sensitive enough for predicting concentrations of Fe, Mn, or other redox-sensitive elements.

Temporal variability in water chemistry

Groundwater and surface water collected at Red Canyon watershed during July 2013 and May 2014 showed minimal seasonal variability in water chemistry. This is illustrated by similar δD and $\delta^{18}O$ isotope ratios (Fig. 3) and similar concentrations of most elements during both July 2013 and May 2014 (Figs. 4, 5). The lack of seasonal variability indicates a stable hydrologic system with relatively long residence times in groundwater. Upland ponds are also important for homogenizing rain and snowmelt in the watershed prior to discharge to streams, as described in the previous work in the watershed (Jin et al. 2012).

Some seasonal differences were observed between July 2013 and May 2014 samples. For example, conductivity and Ca concentrations in groundwater (Fig. 4) tended to be higher in the May samples relative to the July samples. This was unexpected, since the snowmelt recharge should dilute the groundwater chemistry. However, these differences can be explained by cation exchange processes in the groundwater, with lower Na:Ca ratios in May relative to July samples (Supplementary material, Table S1). In the previous work in the watershed, Na:Ca ratios were used as a proxy for groundwater residence times, since the ratio increases with travel distance as Na exchanges for Ca in the subsurface (Lautz and Siegel 2006). May samples, with lower Na:Ca ratios, likely represent "newer" water that has flushed through the groundwater system in response to snowmelt recharge. Flushing of the groundwater system may occur during the snowmelt season, providing less time for cation exchange to occur, and affecting overall groundwater chemistry. Na:Ca ratios could also be affected by water temperature, with cooler water in May samples possibly inhibiting cation exchange relative to warmer water in July. Quantifying residence times in shallow groundwater of mountain streams is important for determining resilience of these systems with climate change. As mountain watersheds transition from snowmelt- to rain-dominated hydrologic systems, the amount of groundwater recharge may decline in the future.

Conclusion

Differences in redox conditions and pH play an important role in controlling concentrations of specific trace elements in groundwater and surface water at Red Canyon watershed, Wyoming. In this investigation, surface water and groundwater samples were collected during July 2013 and May 2014 to evaluate redox chemistry, pH, and trace and major element concentrations. Surface water had high dissolved oxygen concentrations and pH values above 8, whereas groundwater was anoxic with circumneutral pH. Fe and Mn concentrations were elevated in groundwater likely due to reductive dissolution of Fe- and Mn oxides and oxyhydroxides. In contrast, Se, V, and As concentrations were relatively lower in groundwater likely due to pH- and/or redox-driven enhanced sorption to aquifer materials. Groundwater chemistry showed high spatial variability, illustrating the importance of redox zonation, flow pathways, and aquifer properties for controlling water chemistry. There was limited seasonal variability for most measured parameters, suggesting long groundwater residence times in the watershed. This study shows that groundwater–surface water interactions may have important controls on water chemistry in mountain watersheds. These interactions need to be further identified and quantified to understand potential changes to water quality in snowmelt-dominated watersheds under a changing climate.

References

Bauer RL, Siegel DI, Sandvol EA, Lautz LK (2009) Integrating hydrology and geophysics into a traditional geology field course: the use of advanced project options Geological Society of America Special Papers 461:135–154. https://doi.org/10.1130/2009.2461(12)

Carling GT, Fernandez DP, Rudd A, Pazmino E, Johnson WP (2011) Trace element diel variations and particulate pulses in perimeter freshwater wetlands of Great Salt Lake, Utah. Chem Geol 283:87–98

Chapelle FH, Lovley DR (1992) Competitive exclusion of sulfate reduction by Fe(lll)-reducing bacteria: a mechanism for producing discrete zones of high-iron ground water. Ground Water 30:29–36. https://doi.org/10.1111/j.1745-6584.1992.tb00808.x

Dicataldo G, Johnson WP, Naftz DL, Hayes DF, Moellmer WO, Miller T (2011) Diel variation of selenium and arsenic in a wetland of the Great Salt Lake, Utah. Appl Geochem 26:28–36. https://doi.org/10.1016/j.apgeochem.2010.10.011

Dzombak DA, Morel FMM (1990) Surface complexation modeling: hydrous ferric oxide. Wiley, New York

Fanelli RM, Lautz LK (2008) Patterns of water, heat, and solute flux through streambeds around small dams. Ground Water 46:671–687. https://doi.org/10.1111/j.1745-6584.2008.00461.x

Haque S, Ji JF, Johannesson KH (2008) Evaluating mobilization and transport of arsenic in sediments and groundwaters of Aquia aquifer, Maryland. USA J Contam Hydrol 99:68–84. https://doi.org/10.1016/j.jconhyd.2008.03.003

Jin L, Siegel DI, Lautz LK, Otz MH (2009) Transient storage and downstream solute transport in nested stream reaches affected by beaver dams. Hydrol Process 23:2438–2449. https://doi.org/10.1002/hyp.7359

Jin L, Siegel DI, Lautz LK, Mitchell MJ, Dahms DE, Mayer B (2010) Calcite precipitation driven by the common ion effect during groundwater–surface-water mixing: a potentially common process in streams with geologic settings containing gypsum. Geol Soc Am Bull. https://doi.org/10.1130/b30011.1

Jin L, Siegel DI, Lautz LK, Lu ZL (2012) Identifying streamflow sources during spring snowmelt using water chemistry and isotopic composition in semi-arid mountain streams. J Hydrol 470–471:289–301. https://doi.org/10.1016/j.jhydrol.2012.09.009

Lautz LK, Fanelli RM (2008) Seasonal biogeochemical hotspots in the streambed around restoration structures. Biogeochemistry 91:85–104

Lautz LK, Siegel DI (2006) Modeling surface and ground water mixing in the hyporheic zone using MODFLOW and MT3D. Adv Water Resour 29:1618–1633. https://doi.org/10.1016/j.advwatres.2005.12.003

Lautz LK, Siegel DI (2007) The effect of transient storage on nitrate uptake lengths in streams: an inter-site comparison Hydrol Process 21:3533–3548. https://doi.org/10.1002/hyp.6569

Lautz LK, Siegel DI, Bauer RL (2006) Impact of debris dams on hyporheic interaction along a semi-arid stream Hydrol Process 20:183–196. https://doi.org/10.1002/hyp.5910

McMahon PB, Chapelle FH (2008) Redox processes and water quality of selected principal aquifer systems. Ground Water 46:259–271. https://doi.org/10.1111/j.1745-6584.2007.00385.x

Meixner T et al (2016) Implications of projected climate change for groundwater recharge in the western United States. J Hydrol 534:124–138. https://doi.org/10.1016/j.jhydrol.2015.12.027

Nagorski SA, Moore JN (1999) Arsenic mobilization in the hyporheic zone of a contaminated stream. Water Resour Res 35:3441–3450. https://doi.org/10.1029/1999wr900204

Newman B, Tanweer A, Kurttas T (2009) IAEA standard operating procedure for the liquid-water stable isotope analyser. http://www-naweb.iaea.org/napc/ih/documents/other/laser_procedure_rev12.PDF. Accessed 1 May 2019

NOAA (2016) National Oceanic and Atmospheric Administration NCDC. Summary of Monthly Normals, 1981–2010, Station: Lander 11 SSE, WY US GHCND:USW00094078. Report generated 25 March 2016

Parkhurst D, Appelo C (1999) User's guide to PHREEQC (Version 2): a computer program for speciation, batch-reaction, one-dimensional transport, and inverse geochemical calculations. Water Resour Investig Rep 99:312

Siegel D (2008) Reductionist hydrogeology: ten fundamental principles. Hydrol Process 22:4967–4970. https://doi.org/10.1002/hyp.7139

Smedley PL, Kinniburgh DG (2002) A review of the source, behaviour and distribution of arsenic in natural waters. Appl Geochem 17:517–568. https://doi.org/10.1016/S0883-2927(02),00018-5

USEPA (1978) Method 310.1: Alkalinity (Titrimetric, pH 4.5). https://www.nemi.gov/methods/method_summary/5230/. Accessed 1 May 2019

USEPA (1994) Method 200.8, Revision 5.4: Determination of trace elements in waters and wastes by inductively coupled plasma-mass spectrometry. https://www.epa.gov/esam/epa-method-2008-determination-trace-elements-waters-and-wastes-inductively-coupled-plasma-mass. Accessed 1 May 2019

USEPA (1996) Method 1669: Sampling ambient water for trace metals at EPA water quality criteria levels. https://www.epa.gov/sites/production/files/2015-10/documents/method_1669_1996.pdf. Accessed 1 May 2019

USEPA (1997) Method 300.1, Revision 1.0: Determination of inorganic anions in drinking water by ion chromatography. https://www.epa.gov/homeland-security-research/epa-method-3001-revision-10-determination-inorganic-anions-drinking-water. Accessed 1 May 2019

Vázquez-Ortega A et al (2015) Rare earth elements as reactive tracers of biogeochemical weathering in forested rhyolitic terrain. Chem Geol 391:19–32. https://doi.org/10.1016/j.chemgeo.2014.10.016